e-Polymers **2005**, no. 021.

http://www.e-polymers.org
ISSN 1618-7229

Feature article:

Thermo-responsive polymers and hydrogels in tissue engineering

Dirk Schmaljohann

Welsh School of Pharmacy, Cardiff University & Cardiff Institute of Tissue Engineering and Repair (CITER), Redwood Building, King Edward VII Avenue, Cardiff, CF10 3XF, Wales, UK; Fax +44-29-20874536; schmaljohannd@cf.ac.uk

(Received: October 14, 2004; published: March 24, 2005)

Abstract: Various aspects of synthetic polymers and hydrogels in tissue engineering are discussed. A series of graft copolymers based on either *N*-isopropylacrylamide or *N*,*N*-diethylacrylamide as polymer backbone, and on poly(ethylene glycol) as side chain were prepared and characterized. These polymers were then used for the preparation of surface-immobilized hydrogels. The thermo-responsive behaviour was studied on model substrates by ellipsometry. The use of thermo-responsive polymers for *in vitro* studies allows the control of surface properties and thus the stimulation of cell adhesion and detachment through temperature changes. The cellular response was investigated by cultivation of mouse fibroblasts on surface-immobilized, thermo-responsive hydrogels. It was demonstrated that mouse fibroblasts adhere and detach as a function of the temperature, which then could be related to the change in surface properties. The concept is finally extended to the preparation of patterned hydrogels, which were studied by imaging ellipsometry.

Introduction

Tissue engineering aims replacement of damaged or diseased tissues or organs to enable the body to develop or regenerate new functional tissue. This is usually achieved through constructs containing living cells, a three-dimensional porous matrix or scaffold, and bioactive molecules. The constructs should then support cell attachment, proliferation and differentiation [1,2]. There is a large number of potential applications spanning virtually any tissue and organ in the human body, e.g., in bone repair [3-8], cartilage regeneration [9-12], wound healing [13], ocular diseases [14], mandible reconstruction [15], and angiogenesis [16-18]. Materials scientist can provide scaffolds, which exhibit a specific set of properties and functions allowing the regeneration of the desired tissue. Even though every tissue requires a specifically adjusted set of properties, there are certain common features.

Stem cell therapy is one very interesting strategy for tissue regeneration, because it combines the potential of stem cells (SC) to develop into particular functional tissue with the chance of the donor cell coming from the same patient (autologous transplantation), thus an adverse immune response is eliminated. Adult human stem cells are of particular interest, e.g., mesenchymal SC, which can develop into bone,

cartilage tissue and others [19]. The actual development is strongly dependent on a variety of biological regulation systems, e.g. the presence of growth factors, nutrients, cell-cell interaction, cell-matrix interaction, pH, and electrolytes. Some of these factors are only necessary to trigger the development, whereas others are needed as constant stimuli to maintain the functional tissue without dedifferentiation [20].

A large number of treatments require implantation of a scaffold, where the surrounding cells can grow in and generate a functional tissue. In contrast, there is also need to prepare *in vitro* cell culture carrier. For example, autologous stem cell treatment is carried out by the extraction of a small number of stem cells followed by their *in vitro* cultivation to obtain a sufficient large number, which can then be re-implanted with the corresponding scaffold and stimuli. Obviously the *in vitro* systems do not require biodegradability, but well-defined material properties are desired during the whole cell cultivation process.

The scaffold material should comprise an extensive set of properties like biocompatibility, biodegradability, mechanical strength, porosity, potential of entrapment and release of pharmaceutically active agents, and an easy processibility for the clinician. Safety is a critical issue, and similar to new pharmaceuticals, regulatory agencies (e.g., FDA) need to approve the use of the scaffold. Therefore, a large fraction of the research focuses on already approved materials as scaffold, e.g. poly(D,L-lactide) ($P_{DL}LA$), poly(DL-lactic acid-*co*-glycolic acid) (PLGA) and its block-copolymers with poly(ethylene glycol) (PEG) [1,21-23]. Despite this advantage, there is definitely a need for novel materials or smart engineering of the already approved materials to overcome drawbacks of today's system and to treat diseases, where there is currently no treatment available.

Hydrogels can meet all of the above-mentioned properties when choosing the right chemistry. They can provide, e.g., softness, permeability for water, nutrients, metabolites or pharmaceutical active agents, and they show a certain mechanical strength, which enables them to simulate living tissue. Therefore, they are excellent scaffolds for tissue engineering as well as drug delivery devices.

In vitro cell culture of mesenchymal stem cells (MSC) offers various challenges. One of the potential drawbacks occurs upon harvesting MSC from the cell culture carrier. Since MSC's are very adhesive, relatively harsh conditions have to be applied. This is usually carried out by the addition of trypsin as hydrolytic enzyme, which degrades the extracellular matrix (ECM). Besides the fact that this method is very aggressive and cell viability is reduced, it does not conform to GMP regulations, which eliminates potential applications in therapeutics. Thus, there is a need to develop materials, which serve as cell culture carrier and also allow a gentle and GMP compliant harvesting of the cultured cells. One method is the use of stimuli-responsive hydrogels as cell culture, especially when a temperature reduction starting from 37°C is used. This concept has already been applied with poly(*N*-isopropylacrylamide) (PNiPAAm) and copolymers as thermo-responsive material. Okano et al. used surface-grafted PNiPAAm and various copolymers of PNiPAAm as cell culture carriers and tested their potential to prepare transferable cell sheets [24-27]. Addition of acrylic acid as comonomer yields in a fast bio-response to the change in physical properties. Ratner et al. used a plasma polymerization process to prepare a surface-immobilized PNiPAAm hydrogel, which controls cell and protein adhesion [28]. Since non-crosslinked soluble PNiPAAm exhibits a volume phase transition from water-soluble below 32°C to insoluble at higher temperature, the corresponding gels show a transition from fully swollen hydrogel to fully collapsed gel with nearly no water present in the collapsed state. This gives some implication to the use of these

materials in cell culture. If these hydrogels are fully collapsed at 37°C, they behave like a solid substrate, almost similar to conventional polystyrene cell culture carriers. The advantages of hydrogels are completely lost, e.g., permeability in combination with the ability for local rearrangements and a certain mechanical strength.

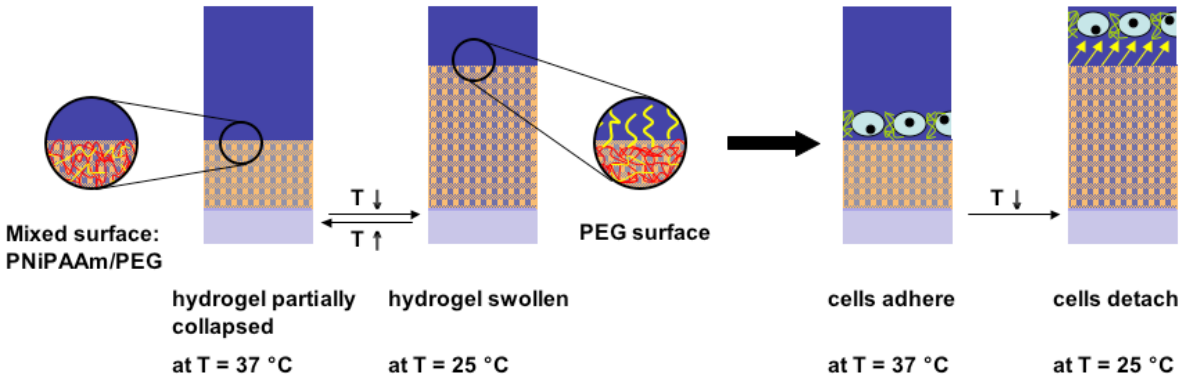

Fig. 1. Thermo-responsive hydrogels and cellular response to change in physical properties of the surface

Thus, it was attempted to prepare a thermo-responsive hydrogel, which maintains hydrogel properties below and above the volume phase transition and which has the potential to control cell adhesion through a thermal stimulus. A large part of this work is dedicated to the physical characterization of these hydrogels, because it is essential to relate a biological response to the inducing physical changes (Fig. 1). However, cell studies will also be reported as proof-of-concept at the end of this paper. After preparation of flat surface-immobilized hydrogels, lateral patterning is used to further improve the hydrogel design; preliminary results of this patterning are also presented within this article. The work focuses on NiPAAm-containing polymers, because their transition behaviour shows greater potential, but DEAAm-containing polymers are also discussed for comparison.

The general rational starts with the synthesis of soluble polymers with the desired transition temperature, which leads to the preparation, characterization and biological investigation of surface-immobilized, thermo-responsive hydrogel (Fig. 1). Experimental procedures are given in separate publications [29-34].

Synthesis and characterization of thermo-responsive polymers

Synthesis

The rational design for the polymer synthesis is to copolymerize a thermo-responsive monomer with a second monomer, which can modulate the responsiveness. Furthermore, a non-linear polymer architecture was thought to be favourable allowing only moderate segment segregation upon the temperature stimulus. *N*-Isopropylacrylamide (NiPAAm) and *N*,*N*-diethylacrylamide (DEAAm) were chosen as thermo-responsive monomers; the corresponding homopolymers have both a volume phase transition, the so-called lower critical solution temperature (LCST), at around 32°C [35]. Ethylene glycol was chosen as second monomer unit, the corresponding poly(ethylene glycol) monomethyl ether monomethacrylate (PEGMA) was used as macromonomer in a free-radical copolymerization. Two different chain lengths of the

macromonomer were selected with either 9 or 45 ethylene glycol units, because the aggregation was expected to be different depending on the chain length. The copolymerization of PEGMA with either NiPAAm or DEAAm (Fig. 2) yields graft copolymers with a thermo-responsive polymer backbone and PEG side chains [29]. The choice of the polymer chemistry was motivated by the expected biocompatibility, which is for PEG already well reported [36], and the potential to fine-tune the volume phase transition by adding comonomers to PNiPAAm or PDEAAm, respectively. The free-radical initiator ACPA (4,4'-azobis(4-cyanopentanoic acid) was chosen in order to conduct the copolymerization in various hydrophilic solvents including water [37]. It is known that hydrophilic comonomers tend to shift the LCST of PNiPAAm (32 - 33°C) towards higher temperatures. Hydrophobic comonomers have the opposite effect [35].

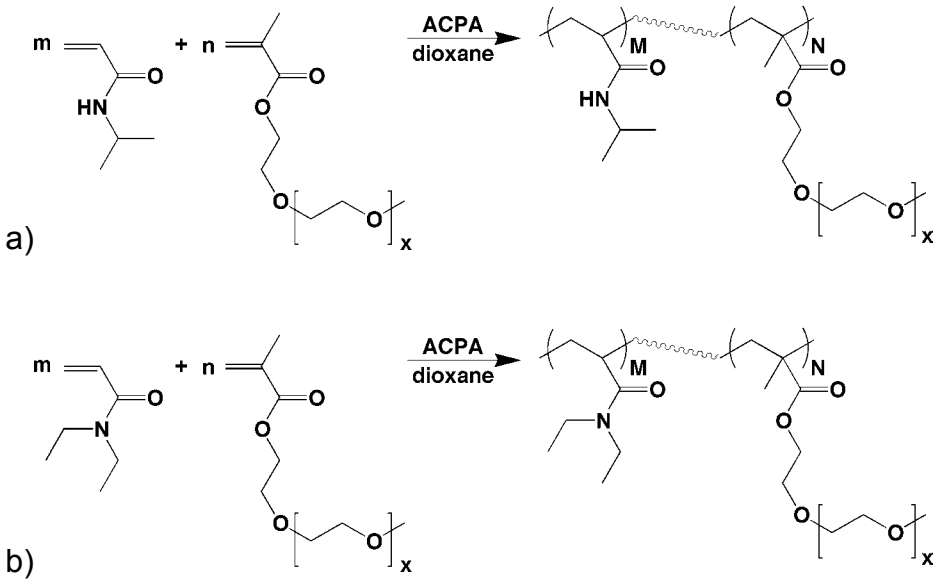

Fig. 2. Synthetic scheme for the preparation of thermo-responsive graft copolymers using the macromonomer method; a) NiPAAm containing copolymers, b) DEAAm containing copolymers; ACPA = 4,4'-azobis(4-cyanopentanoic acid), x = 8, 44

Thus, PEG is shifting the LCST of PNiPAAm and PDEAAm, respectively, towards higher values. A series of graft copolymers was synthesised and characterized. The molecular weight ranged between 15 000 and 25 000. Several other groups have also studied PNiPAAm/PEG copolymers with different polymer architecture. Maeda et al. [38], Virtanen et al. [39] and Topp et al. [40] synthesised block-copolymers, whereas Virtanen et al. also described the preparation of graft copolymers by the 'grafting-onto' method [41,42]. The block-copolymers have a volume phase transition around 32°C, but the graft copolymers exhibit a shift in the transition temperature T_{tr} towards higher values similar to our observations.

Volume phase transition or LCST behaviour

The LCST is defined as the minimum in a phase diagram. Even though PNiPAAm shows little influence on the transition temperature T_{tr} as a function of molecular weight or concentration, the data is reported as the temperature of the volume phase transition T_{tr}. T_{tr} was determined by three different methods: UV/Vis turbidity measurements (or cloud point measurement, determined as inflection point), capillary flow

viscometry (inflection point) and DSC measurements (peak maximum) [35]. These methods span two orders of magnitude in concentration, and one can observe a minor concentration effect with decreasing T_{tr} on increasing concentration. Surprisingly, the two different series of copolymers (with different PEG chain length) show a similar volume phase transition when plotting T_{tr} against the mole ratio of EG units but not against the mole ratio of comonomers, which is usually used to describe the LCST behaviour of NiPAAm copolymers with low-MW comonomers [43]. The macromonomer PEGMA effects the phase transition of, e.g., PNiPAAm relative to the mole ratio of ethylene glycol (EG) units. Fig. 3 gives a plot of T_{tr} as function of the mole ratio of EG for the NiPAAm-containing polymers as example. A similar behaviour was found for the DEAAm-containing graft copolymers.

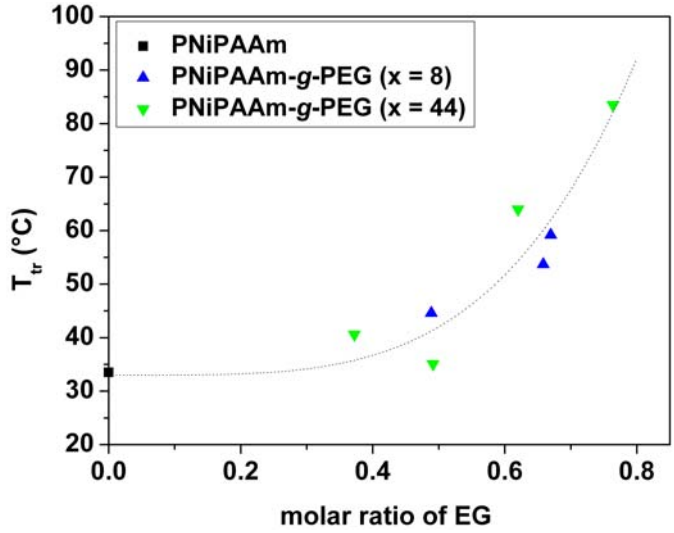

Fig. 3. Plot of T_{tr} of PNiPAAm graft copolymers (determined by UV/Vis turbidity measurements, 400 and 600 nm) vs. mole ratio of EG in PEGMA, x = 8, 44 (compare Fig. 2)

This unusual behaviour indicates an interaction of the PEG chains, which goes beyond the direct influence of the neighbouring groups. The observation is different to results based on PNiPAAm-*b*-PEG block copolymers, which do not show any shift in the LCST [38-40]. Further studies, however, need to be carried out to fully describe this behaviour. Four candidates were selected from this series of graft copolymers for further experiments. These polymers show a transition temperature in the range of 37°C or below, which finally would allow going through the volume phase transition when switching the temperature between room temperature and body/cell culture temperature. Tab. 1 gives the composition and the T_{tr}'s of the selected polymers.

As expected, the transition temperature decreases when increasing the concentration to 1 mg/mL and stays then roughly at the same temperature. The variations in the obtained T_{tr} values are also due to the different data evaluation methods, but the general trend is consistent with PNiPAAm homopolymer [35]. The variation in T_{tr} of P1 compared to P2 and P3 compared to P4, respectively, can be explained with experimental errors in the determination method due to broad transitions and in the NMR measurements due to partial signal overlap (compare Fig. 3). In any case, a PEG content of 10 - 20 wt.-% should be sufficient to modulate the surface properties of the corresponding surface-immobilized hydrogels while staying within the settings

of the planned cell culture experiments. Tab. 2 summarizes the volume phase transition behaviour further with respect to addition of electrolytes to the system.

The transition temperature decreases upon addition of electrolytes as in phosphate buffer saline (PBS) solution, which is conform to literature data [44]. There is no major difference in the results of measurements in PBS solution compared to a typical cell culture medium (RPMI) with added fetal calf serum (FCS). Finally, in RPMI medium, the volume phase transition of all polymers is below 37°C. The four soluble polymers were then used for the plasma immobilization procedure to prepare surface-immobilized, thermo-responsive hydrogels.

Tab. 1. Composition and LCST (T_{tr}) of the thermo-responsive graft copolymers

No.	Comonomer mole ratio [a]				T_{tr} in deionized water in °C		
	NiPAAm	DEAAm	PEGMA (x = 8)	PEGMA (x = 44)	UV/Vis [b]	viscometry [c]	DSC [d]
P1	0.99	-	-	0.01	40.7	36.0	36.7
P2	0.98	-	-	0.02	35.1	34.0	33.9
P3	-	0.99	-	0.01	38.8	36.4	-
P4	-	0.96	0.04	-	37.7	35.6	-

[a] Determined by ^{1}H NMR. [b] Inflection point, c = 0.1 mg/mL, evaluated wavelengths: 400 and 600 nm. [c] Inflection point, c = 1 mg/mL. [d] Peak maximum, c = 10 mg/mL.

Tab. 2. T_{tr} of the thermo-responsive graft copolymers in various aqueous media

No.	wt.-% PEG	T_{tr} (UV/Vis turbidity) [a] in °C		
		DI water	PBS solution	RPMI + 10% FCS
P1	19	40.7	38.0	36.3
P2	23	35.1	34.4	34.3
P3	9	38.8	34.3	33.7
P4	11	37.7	34.4	34.4

[a] Evaluated wavelengths: 400 and 600 nm; DI water: deionized water; PBS solution: phosphate buffer saline solution; RPMI: cell culture medium; FCS: fetal calf serum.

Surface-immobilized, thermo-responsive hydrogels

Low-pressure argon plasma immobilization technique

Plasma exposure was utilized for crosslinking and immobilization of the spin-coated polymers layer. Nitschke et al. have demonstrated that this approach can be used for the immobilization of various classes of polymers (e.g., poly(vinylpyrrolidone) (PVP), poly(acrylic acid) (PAA), poly(ethyleneimine) (PEI), PNiPAAm) [34,45,46]. Low-pressure argon plasma generates UV light of high intensity, which causes random chain scission and recombination in the polymer chain. Thus the exposure time has to be controlled for an effective immobilization without major polymer degradation. The sequence of reaction steps towards the final hydrogel sample is given in Fig. 4.

A silicon wafer, which is coated with a PTFE-like layer, is exposed to oxygen plasma for improved wettability and compatibilization with the polymer. Then, the polymer is spin-coated from chloroform solution (0.5 wt.-%), exposed to the plasma and subsequently rinsed with chloroform for removal of non-bonded polymer. The results are reproducible with respect to dry film thickness, as long as spin-coating and plasma conditions are kept constant.

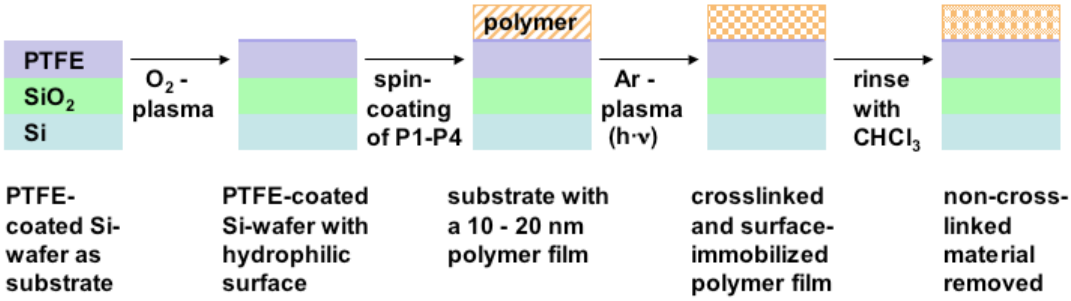

Fig. 4. Plasma immobilization and crosslinking procedure (also layer model for ellipsometry data fit)

ATR-FTIR measurements before and after plasma exposure showed that no change in the surface chemistry was observed indicating random crosslinking without major degradation [34]. The plasma process is a very efficient way of polymer immobilization, which does not require any particular polymer chemistry. The advantage for this particular series of experiments lays in the fact that the soluble model polymers can be directly used as precursors. Thus the measured T_{tr} values are expected to be close to the transition points of the corresponding hydrogels. Any use of a chemical crosslinker would have a potential effect on the transition temperature. One limitation of this process is the film thickness, which cannot exceed ≈ 20 nm, because otherwise surface immobilization would not be achieved anymore. For thicker films, either an e-beam exposure can be used or a layer-by-layer approach with plasma exposure. The latter approach also allows the preparation of lateral and vertical heterogeneous hydrogels. Tab. 3 gives the obtained film thicknesses of the immobilized hydrogels.

Temperature-dependent swelling behaviour of the surface-immobilized hydrogels

Once the crosslinked and immobilized hydrogel is taken out of the plasma chamber, it starts to swell due to uptake of water through moisture. Therefore, a conventional measurement of the film thickness always gives a value for a partially swollen film. All immobilized hydrogels were intensively studied by temperature-dependent ellipsometry. Ellipsometry is a fast and non-invasive method for characterizing the properties of polymers at the interface and in thin films. Variable angle spectroscopic ellipsometry (VASE) was applied as experimental technique [47]. The experimental data is expressed as relative phase shift Δ and relative amplitude ratio tan Ψ. It can be modelled in order to obtain the film thickness *d* and the refractive index *n*. Knowledge of n_{H2O} and $n_{polymer}$ is used to calculate the degree of swelling (DS) [34]. Fig. 5 indicates the temperature-dependent swelling and collapsing behaviour of the hydrogel, and it also shows the layer model that was used for fitting the experimental data. The measurements were carried out in a solid-liquid cell connected to a thermostat and the temperature was cycled between 23 and 55°C at rate of ca. 0.25 K/min. This

rate corresponds to the cooling rate as applied in the cell culture experiment (Fig. 11). Therefore, the changes in film thickness *d* can be related to the biological response. This time scale of changes in *d* or DS is denoted as 'dynamic swelling' in order to distinguish it from an equilibrium situation. Fig. 5 also indicates the 'equilibrium swelling', when the sample is stored under water for a longer time and its film thickness is monitored as a function of time [34].

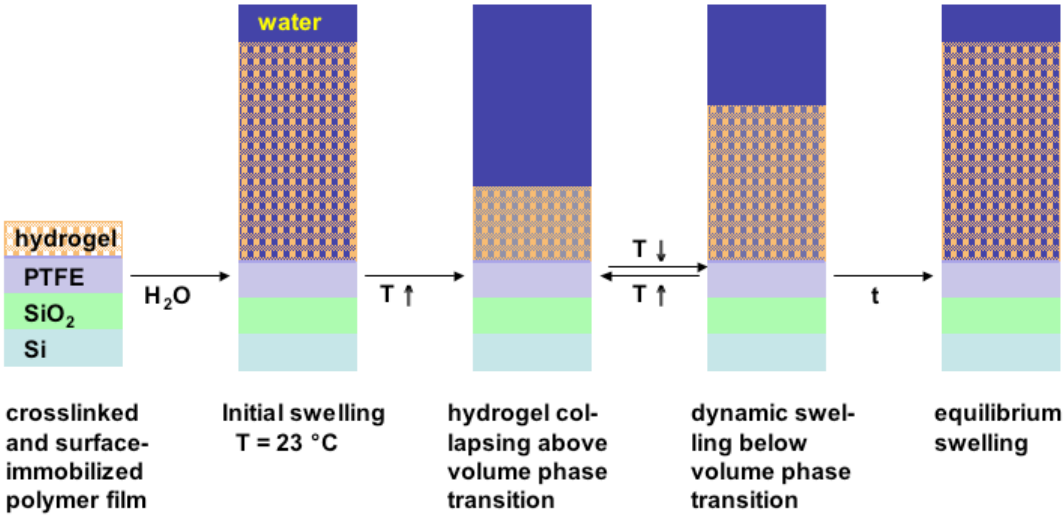

Fig. 5. Scheme of the thermo-responsive swelling and collapsing of the surface-immobilized hydrogels (also layer model for ellipsometry)

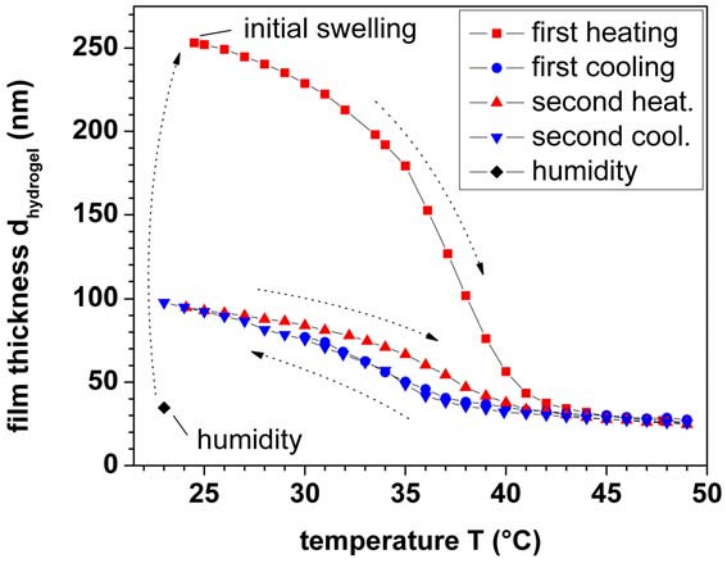

Fig. 6. Film thickness $d_{hydrogel}$ of P1 vs. *T*; 1st and 2nd heating-cooling cycles; data point ♦ measured before immersion into water at 40 - 50% relative humidity

The film thickness (*d*) relates to the degree of swelling (DS) by the following equation:

$$DS = d_{hydrogel}/d_{dry} \quad (1)$$

The difference between initial and dynamic swelling becomes obvious when examining the hydrogel film thickness as function of temperature. Fig. 6 shows a plot of

$d_{hydrogel}$ vs. T for the first and second heating/cooling cycles of P1; the curves for P2 - P4 are similar, their data are given in Tab. 3.

The swelling behaviour of the immobilized hydrogels becomes reproducible after the initial heating above the volume transition, the so-called lower gel transition temperature (LGTT). As pointed out earlier, this is not an equilibrium state, however, the equilibrium swelling occurs on a different time scale, 1 to 2 orders of magnitude larger compared to the dynamic swelling [34]. The substantially lower degree of swelling below the LGTT in the dynamic range is probably due to physical crosslinks and entanglements, which need much more time to be reversed. In the dynamic range, the heating and cooling curves show a hysteresis, which also indicates the non-equilibrium situation. It is noteworthy that DS at 42°C varies between 2 and 8 for the different hydrogels, compared to DS of 4 to 13 at 25°C, respectively. Furthermore, the two cooling scans in Fig. 6 are almost identical, which indicates a small error on repeated measurements of the same sample. The variation on ellipsometry measurements of different spots on the same sample was similarly small. Thus, the prepared hydrogel switches between fully swollen and partially collapsed, or between all-hydrophilic and amphiphilic. It is important to note that the thermo-responsive gels maintain certain hydrogel properties above the LGTT.

Tab. 3. Film thickness (d_{dry}) and degree of swelling (DS) of the surface-immobilized hydrogels in water

No.	Dry film thickness d_{dry}/nm	Degree of swelling (DS) in DI water			
		23°C humidity [a)]	23°C initial swelling	42°C dynamic swelling	25°C dynamic swelling
P1	15.2	2.28	16.6	1.97	6.05
P2	11.3	2.07	14.0	3.45	6.81
P3	15.6	1.61	5.58	2.24	3.91
P4	6.5	3.27	14.0	8.00	12.8

[a)] Measured before immersion into water at 40 - 50% relative humidity.

A comparison of the volume phase transition of the polymers in solution with the corresponding hydrogels shows that the hydrogel transitions are much broader compared to the sharp transitions of the solutions (Fig. 7). In particular, the LGTT's of the DEAAm-containing hydrogels (P3, P4, Fig. 7b) exhibit a nearly linear response to the change in temperature. This difference compared to the NiPAAm-containing hydrogel (P1, P2, Fig. 7a) may be due to the different hydrogen bonding capability: the NH of the primary amide of NiPAAm can act as H-bond donor, whereas the secondary amide of DEAAm can only act as H-bond acceptor. The broader transitions of the immobilized hydrogels compared to the polymer solutions can possibly be explained by kinetic effects, since the measurement are not conducted in equilibrium and physical entanglements are opened. The very broad transitions of the DEAAm-containing hydrogels make the determination of the LGTT difficult. Therefore, the LGTT's of P3 and P4 indicate only roughly the transition, which is in all cases determined as inflection point of the $d_{hydrogel}$-T-plot (Tab. 4) [48].

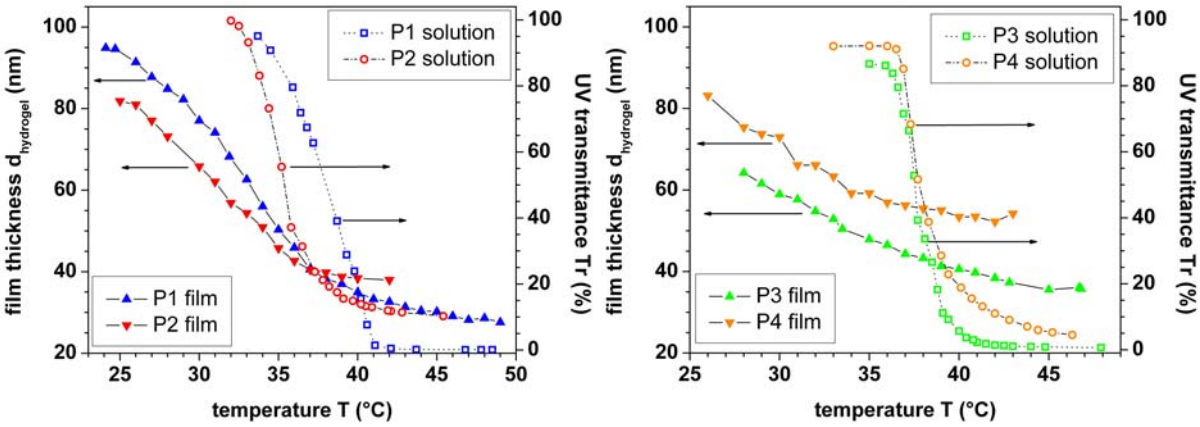

Fig. 7. Comparison of the transitions of the hydrogel with those of a polymer solution: film thickness $d_{hydrogel}$ and UV transmittance vs. temperature

Tab. 2 already demonstrated that the addition of electrolytes to water causes shift of T_{tr} towards lower values. The same observation can be made when studying the corresponding hydrogels as shown for P1 as an example (Tab. 4, Fig. 11). In addition, the crosslinking procedure causes a decrease in the volume phase transition temperature. In conclusion, the combination of crosslinking and addition of electrolytes leads to a decrease of the transition temperature by 5 - 8 K compared to the soluble starting polymer in DI water. More important, since this behaviour is very consistent, the T_{tr} data from the polymer solution in DI water can be used as a fast route to identify potential candidates for thermo-responsive cell culture carrier.

Tab. 4. Volume phase transition in the hydrogels and polymer solutions in DI water and in PBS solution (DI water: deionized water; PBS solution: phosphate buffer saline solution; T_{tr}: temperature of the volume phase transition; LGTT: lower gel transition temperature)

No.	DI water			PBS solution		
	T_{tr} [a] in °C cooling	LGTT [b] in °C heating	LGTT [b] in °C cooling	T_{tr} [a] in °C cooling	LGTT [b] in °C heating	LGTT [b] in °C cooling
P1	40.7	37	35	38.0	35	≈32
P2	35.1	35	33	34.4	-	-
P3	38.8	≈35	≈32	34.3	-	-
P4	37.7	≈34	≈31	34.4	-	-

[a] UV/Vis turbidity; inflection point, 400 and 600 nm. [b] Inflection point of the $d_{hydrogel}$-T-plot.

The transition with change in DS can also be related to a switch in the surface energy, which can be studied by contact angle measurements. The P2 hydrogel, which has the highest PEG content of the four polymers, has been studied with static inverse contact angle using the captive bubble method [49] above and below the LGTT. The resulting contact angle is compared to that of a PNiPAAm hydrogel, prepared with the same method (Tab. 5) [33].

Tab. 5. Contact angles of P2 and PNiPAAm in DI water (static contact angle, measured by captive bubble method)

	Contact angle		wt.-% PEG	T_{tr} in °C
	at 28°C	at 42°C		
PNiPAAm	27°	62°	0	32
P2	32°	41°	23	35

Again, the contact angle measurements indicate the differences between hydrogels based on either a PNiPAAm homopolymer or a PNiPAAm-*g*-PEG graft copolymer, respectively. Below the transition point, there is little difference between P2 and PNiPAAm, however above the volume phase transition, the PNiPAAm hydrogel becomes relatively hydrophobic with a contact angle of 62°. In contrast, P2 shows only an increase in the contact angle by 9°, clearly indicating a mixed surface of PEG and PNiPAAm above the transition point. The question, whether P2 exposes a PEGylated surface – as indicated in Fig. 1 – cannot be answered from the contact angle measurements.

The satisfactory position of the LGTT for the P1 hydrogel in combination with a relatively sharp transition and a large change in DS between swollen and (partially) collapsed state led to the choice of P1 as candidate for further experiments on hydrogel patterning and cell culture, which will be discussed in the following sections.

Patterning of hydrogels

Photolithographic patterning of the thermo-responsive hydrogels

The preparation of heterogeneous hydrogels offers further potential for precise localizing of the immobilized cells, or co-localizing of different cell types. Especially the use of PEG in a patterning process allows avoiding non-desired cell adhesion [50-54], but also PHEMA and PNiPAAm hydrogels have been patterned already [55-58]. Photolithographic and softlithographic techniques have been used in the patterning of hydrogels and also two-photon processes have been applied [59]. Since the plasma process induces polymer crosslinking, the same procedure can also be utilized for a photolithographic process leading towards patterned hydrogels (Fig. 8). The UV exposure has to be carried out through a mask, which gives crosslinking only in selected regions of the polymer film.

The overall process yields a negative-tone image of the mask, because it causes a crosslinking of the exposed parts and the non-exposed parts are removed by a rinsing step afterwards. A TEM grid is used as mask to give a proof-of-principle for the lithographic process [60]. The resolution is 60 µm, however, other masks are expected to give much higher resolution.

Characterization of the patterned hydrogels

Fig. 9 shows a microscopic image of the patterned hydrogel after the rinsing step (Fig. 8), which proves the success of the patterning process. Further characterization of the patterned hydrogel was carried with imaging ellipsometry. In contrast to conventional ellipsometry, the imaging ellipsometry set-up combines a typical ellipso-

metry experiment with an objective and a CCD camera as detector, where each pixel on the CCD camera allows a separate ellipsometry experiment [61-63]. Data processing gives then a 3D-profile of, e.g., Δ values with a resolution of 1 - 2 µm, as shown in Fig. 10. The height of hydrogel film can be followed through the Δ profile, because Δ goes along with the film thickness [34,60].

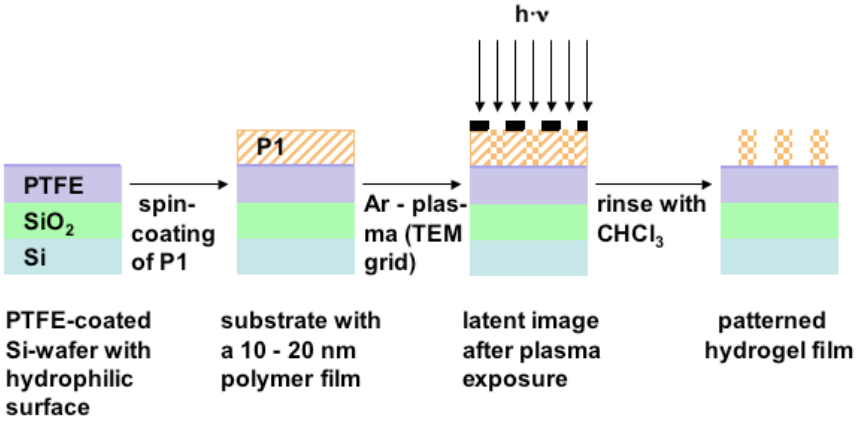

Fig. 8. Photolithographic process for the preparation of patterned hydrogels by plasma exposure

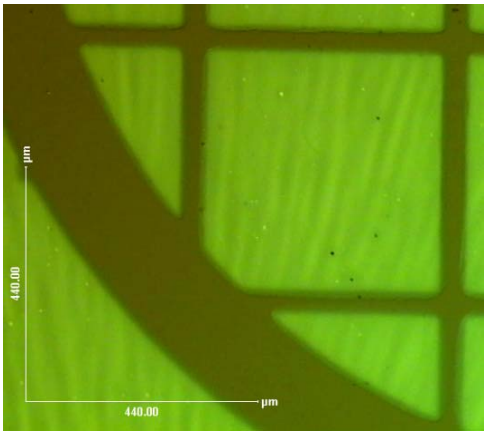

Fig. 9. Optical microscopy image of the patterned hydrogel P1 (scale bar: 440 µm)

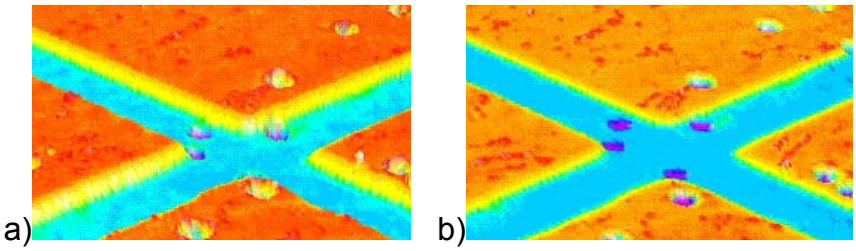

Fig. 10. 3D-Profile of Δ of patterned P1 in DI water at different temperatures, obtained by imaging ellipsometry; a) 25°C, b) 35°C [64]

It is noteworthy that the resolution is maintained after swelling in DI water. Thus only swelling in *z*-direction occurs. The patterned hydrogel will be exploited in the future with cell culture and release studies of pharmaceutical active agents. Before using

patterned hydrogels, the cell response has to be tested on flat substrates, which will be presented in the following section.

Application as thermo-responsive cell culture carrier

For the cell culture experiments, glass slides were prepared in the same way as described in Fig. 4 using P1 as polymer and employing the same plasma conditions as for the silicon wafers. The hydrogel shows a volume phase transition between 32 and 34°C with a degree of swelling DS = 2.4 in PBS solution (Fig. 11). This gives the desired change in surface properties along with a relatively sharp volume phase transition.

L929 mouse fibroblasts were cultivated on the hydrogel for several days in RPMI medium (+ 10% FCS). The cells adhere well, spread and proliferate on the surface at 37°C. Thus, the hydrogel is suitable as cell culture carrier, and the gels were confirmed to be non-toxic and cell adhesion was not reduced due to the PEG content. After the cell cultivation was finished, the temperature was reduced at a rate of *c*. -0.1 K/min and the response of the cells was followed by microscopy. Fig. 11 shows the detachment of the fibroblasts after reduction of the temperature by 3 K [32].

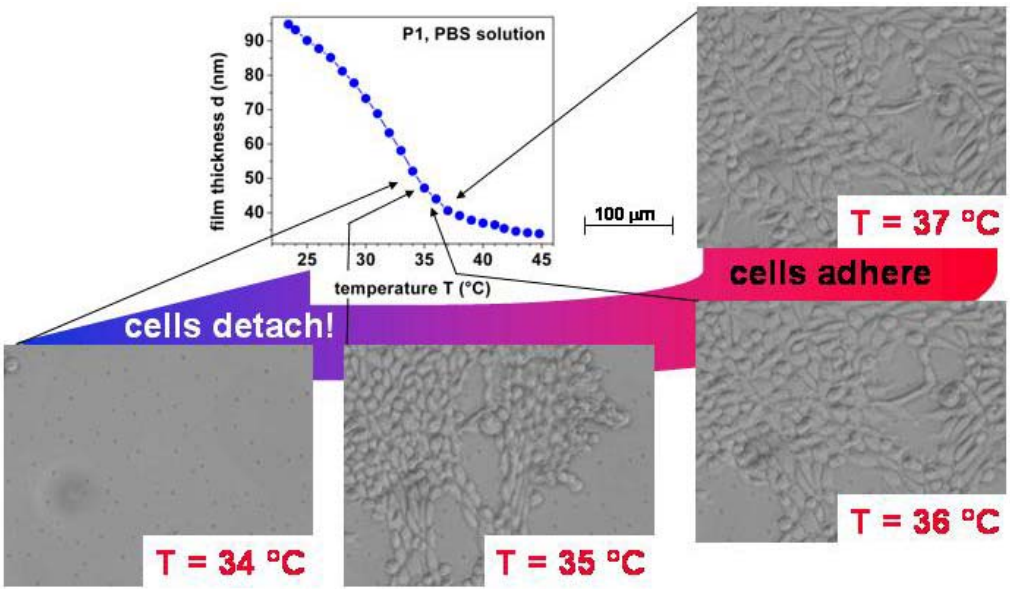

Fig. 11. Temperature-dependent ellipsometry of P1 in PBS (hydrogel on Si-wafer, cooling scan) and micrographs of L929 mouse fibroblasts at various temperatures during cell detachment (hydrogel on glass)

The mouse fibroblasts detach as sheets of cells from the substrate, and the detachment is completed within 20 min. Thus, it can be considered as fast responding hydrogel, similar to experiments by Okano et al. [24]. The main difference is that almost 20 wt.-% of PEG is incorporated, and the LGTT is still below 37°C. This unexpected observation can possibly be attributed to a strong interaction of PEG with PNiPAAm above the LGTT, which is due to the graft architecture of the starting material. This would then lead to the formation of a mixed surface (PNiPAAm/PEG) at 37°C and a PEGylated surface at lower temperature. A switch from mixed surface to PEGylated surface would then induce the detachment by minimizing the cell-

substrate interactions as indicated in Fig. 1 [65]. Furthermore, the degree of swelling at 37°C is *c*. 2.7, indicating hydrogel properties under cell culture conditions [36].

Conclusions and future aspects

The discussed work went from the synthesis and characterization of thermo-responsive graft copolymers, over the preparation of the corresponding surface-immobilized hydrogels, towards the patterning of these hydrogels and the evaluation of its cell adhesion behaviour.

The application of synthetic materials in biomedical applications requires a careful characterization of the material in order to relate the physical properties to the biological response. Even though further characterization of the described polymers and hydrogels is necessary, a relation between the physical properties of the surface-immobilized hydrogels like LGTT, degree of swelling, contact angle and cell-substrate interaction can be established to the achieved control over cell adhesion and detachment of the mouse fibroblasts.

During these studies, one polymer (P1) was chosen as candidate for the intended application as thermo-responsive cell culture carrier. This selection process out of a large number of soluble polymers to a few candidates, which progress to the hydrogel preparation, was shown to be a very efficient method. However, further candidates need to be identified to further improve the material. This includes the addition of other functionalities for either a pH-response or the immobilization of, e.g., growth factors. But it is also necessary to achieve more control over the synthesised polymers with respect to molecular weight, molecular weight distribution and comonomer composition. Thus, controlled radical copolymerization is another avenue to a better relation of properties to bio-response.

In conclusion, stimuli-responsive polymers are gaining recognition in biomedical applications, not only in regenerative medicine, but also as ‘smart’ drug carrier and drug delivery systems and in general in the field of nanomedicines [66,67].

Acknowledgement: I am very grateful to a large number of colleagues for their support and critical discussion of this work, in particular thanks to Prof. B. I. Voit and Dr. C. Werner. I also thank my collaborators and students, who were involved in the various aspects of this work: Dr. M. Nitschke, Dr. J. Oswald, Dr. K.-J. Eichhorn, S. Gramm, N. Tarek El Tahan, Dr. S. Zschoche, C. Hung, L. Dieudonné. Furthermore, I am grateful to Dr. L. Izzo for revision of the manuscript.

[1] Hou, Q.; De Bank, P. A.; Shakesheff, K. M.; *J. Mater. Chem.* **2004**, *14*, 1915.

[2] Langer, R.; Tirrell, D. A.; *Nature* **2004**, *428*, 487.

[3] Bensaid, W.; Triffitt, J. T.; Blanchat, C.; Oudina, K.; Sedel, L.; Petite, H.; *Biomaterials* **2003**, *24*, 2497.

[4] Lutolf, M. P.; Weber, F. E.; Schmoekel, H. G.; Schense, J. C.; Kohler, T.; Müller, R.; Hubbell, J. A.; *Nature Biotech.* **2003**, *21*, 513.

[5] Burdick, J. A.; Anseth, K. S.; *Biomaterials* **2002**, *23*, 4315.

[6] Burdick, J. A.; Mason, M. N.; Hinman, A. D.; Thorne, K.; Anseth, K. S.; *J. Controlled Release* **2002**, *83*, 53.

[7] Yang, X. B.; Tare, R. S.; Partridge, K. A.; Roach, H. I.; Clarke N. M.; Howdle, S. M.; Shakesheff, K. M.; Oreffo, R. O.; *J. Bone Min. Res.* **2003**, *18*, 47.

[8] Rowley, J. A.; Madlambayan, G.; Mooney, D. J.; *Biomaterials* **1999**, *20*, 45.

[9] Holland, T. A.; Tabata, Y.; Mikos, A. G.; *J. Controlled Release* **2003**, *91*, 299.

[10] Stile, R. A.; Burghardt, W. R.; Healy, K. E.; *Macromolecules* **1999**, *32*, 7370.

[11] Chenite, A.; Chaput, C.; Wang, D.; Combes, C.; Buschmann, M. D.; Hoemann, C. D.; Leroux, J. C.; Atkinson, B. L.; Binette, F.; Selmani, A.; *Biomaterials* **2000**, *21*, 2155.

[12] Anseth, K. S.; Metters, A. T.; Bryant, S. J.; Martens, P. J.; Elisseeff, J. H.; Bowman, C. N.; *J. Controlled Release* **2002**, *78*, 199.

[13] Stevens, P.; Wood, E. J.; Raxworthy, M. J.; *Wound Rep. Reg.* **1996**, *4*, 393.

[14] Kinoshita, S.; Nakamura, T.; *Artif. Organs* **2004**, *28*, 22.

[15] Gronthos, S.; *Lancet* **2004**, *364*, 735.

[16] Elcin, Y. M.; Dixit, V.; Gitnick, T.; *Artif. Organs* **2001**, *25*, 558.

[17] Hall, H.; Baechi, T.; Hubbell, J. A.; *Microvasc. Res.* **2001**, *62*, 315.

[18] Mallery, S. R.; Pei, P.; Kang, J. C.; Zhu, G. Z.; Ness, G. M.; Schwendeman, S. P.; *Carcinogenesis* **2000**, *21*, 1647.

[19] Pittenger M. F.; Mackay, A. M.; Beck, S. C.; Jaiswal, R. K.; Douglas, R.; Mosca, J. D.; Moorman, M. A.; Simonetti, D. W.; Craig, S.; Marshak, D. R.; *Science* **1999**, *284*, 143.

[20] Minuth, W. W.; Strehl, R.; Schumacher, K.; "*Von der Zellkultur zum Tissue engineering*", Pabst Science Publishers, Lengerich **2002**.

[21] Yang, X. B.; Tare, R. S.; Partridge, K. A.; Roach, H. I.; Clarke, N. M.; Howdle, S. M.; Shakesheff, K. M.; Oreffo, R. O.; *J. Bone Min. Res.* **2003**, *18*, 47.

[22] Han, D.; Hubbell, J. A.; *Macromolecules* **1997**, *30*, 6077.

[23] Jeong, B.; Bae, Y. H.; Lee, D. S.; Kim, S. W.; *Nature* **1997**, *388*, 860.

[24] Ebara, M.; Yamato, M.; Hirose, M.; Aoyagi, T.; Kikuchi, A.; Sakai, K.; Okano, T.; *Biomacromolecules* **2003**, *4*, 344.

[25] Ebara, M.; Yamato, M.; Aoyugi, T.; Kikuchi, A.; Sakai, K.; Okano, T.; *Biomacromolecules* **2004**, *5*, 505.

[26] Akiyama, Y.; Kikuchi, A.; Yamato, M.; Okano, T.; *Langmuir* **2004**, *20*, 5506.

[27] Tsuda, Y.; Kikuchi, A.; Yamato, M.; Sakurai, Y.; Umezu, M.; Okano, T.; *J. Biomed. Mater. Res. Part A* **2004**, *69A*, 70.

[28] Cheng, X. H.; Wang, Y. B.; Hanein, Y.; Bohringer, K. F.; Ratner, B. D.; *J. Biomed. Mater. Res. Part A* **2004**, *70A*, 159.

[29] Schmaljohann, D.; Gramm, S.; *Polym. Prepr.* **2002**, *43*, 758.

[30] Gramm, S.; Komber, H.; Schmaljohann, D.; *J. Polym. Sci., Part A: Polym. Chem.* **2005**, *43*, 142.

[31] Schmaljohann, D.; Oswald, J.; Jørgensen, B.; Nitschke, M.; Beyerlein, D.; Werner, C.; *Polym. Mater. Sci. Eng.* **2003**, *89*, 255.

[32] Schmaljohann, D.; Oswald, J.; Jørgensen, B.; Nitschke, M.; Beyerlein, D.; Werner, C.; *Biomacromolecules* **2003**, *4*, 1733.

[33] Schmaljohann, D.; Beyerlein, D.; Nitschke, M.; Zschoche, S.; Werner, C.; *Polym. Mater. Sci. Eng.* **2003**, *88*, 551.

[34] Schmaljohann, D.; Beyerlein, D.; Nitschke, M.; Werner, C.; *Langmuir* **2004**, *20*, 10107.

[35] Schild, H. G.; *Prog. Polym. Sci.* **1992**, *17*, 163.

[36] Harris, J. M., editor; "*Poly(ethyleneglycol) chemistry: biotechnical and biomedical applications*", Plenum Press, New York **1992**.

[37] ACPA was purchased from FLUKA and used as received; NiPAAm was obtained from ACROS and recrystallized from hexane; both PEGMAs were purchased from Aldrich and used as received; DEAAm was synthesized by Schotten-Baumann reaction.

[38] Maeda, Y.; Taniguchi, N.; Ikeda, I.; *Macromol. Rapid Commun.* **2001**, *22*, 1390.

[39] Virtanen, J.; Holappa, S.; Lemmetyinen, H.; Tenhu, H.; *Macromolecules* **2002**, *35*, 4763.

[40] Topp, M. D. C.; Dijkstra, P. J.; Talsma, H.; Feijen, J.; *Macromolecules* **1997**, *30*, 8518.

[41] Virtanen, J.; Baron, C.; Tenhu, H.; *Macromolecules* **2000**, *33*, 336.

[42] Virtanen, J.; Tenhu, H.; *Macromolecules* **2000**, *33*, 5970.

[43] Kuckling, D.; Adler, H.-J. P.; Arndt, K.-F.; Ling, L.; Habicher, W. D.; *Macromol. Chem. Phys.* **2000**, *201*, 273.

[44] Zhang, X.; Hu, Z.; Li, Y.; *J. Appl. Polym. Sci.* **1997**, *63*, 1851.

[45] Nitschke, M.; Menning, A.; Werner, C.; *J. Biomed. Mater. Res.* **2000**, *50*, 340.

[46] Nitschke, M.; Zschoche, S.; Baier, A.; Simon, F.; Werner, C.; *Surf. Coat. Tech.* **2004**, *185*, 120.

[47] Debe, M. K.; Field, D. R.; *J. Vac. Sci. Techn.* **1991**, *A9*, 1265.

[48] The inflection point was determined as minimum of the 1st derivative of the $d_{hydrogel}$-*T*-plot. For P3 and P4, the middle value in the plateau region was taken as gel transition temperature.

[49] Grundke, K.; Werner, C.; Pöschel, K.; Jacobasch, H. -J.; *Colloid Surf. A* **1999**, *156*, 19.

[50] Sirkar, K.; Pishko, M. V.; *Anal. Chem.* **1998**, *70*, 2888.

[51] Koh, W.-G; Itle, L. J.; Pishko, M. V.; *Anal. Chem.* **2003**, *75*, 5783.

[52] Koh, W.-G.; Pishko, M.; *Langmuir* **2003**, *19*, 10310.

[53] Revzin, A.; Tompkins, R. G.; Toner, M.; *Langmuir* **2003**, *19*, 9855.

[54] Suh, K.Y.; Seong, J.; Khademhosseini, A.; Laibnis, P. E.; Langer, R.; *Biomaterials* **2004**, *25*, 557.

[55] Chiellini, F.; Bizarri, R.; Ober, C. K.; Schmaljohann, D.; Solaro, R.; Chiellini, E.; *Macromol. Rapid Commun.* **2001**, *22*, 1284.

[56] Chiellini, F.; Bizarri, R.; Ober, C. K.; Schmaljohann, D.; Yu, T.; Saltzman, W. M.; Solaro, R.; Chiellini, E.; *Macromol. Symp.* **2003**, *197*, 369.

[57] Kuckling, D.; Hoffmann, J.; Plötner, M.; Ferse, D.; Kretschmer K.; Adler, H.-J. P.; Arndt, K.-F.; Reichelt, R.; *Polymer* **2003**, *44*, 4455.

[58] Harmon, M. E.; Tang, M.; Frank, C. W.; *Polymer* **2003**, *44*, 4547.

[59] Yu, T.; Ober, C. K.; *Biomacromolecules* **2003**, *4*, 1126.

[60] Schmaljohann, D.; Nitschke, M.; Schulze, R.; Werner, C.; Eing., A.; Eichhorn, K.-J.; *Langmuir* **2005**, *21*, 2317.

[61] Hönig, D.; Möbius, D.; *J. Phys. Chem.* **1991**, *95*, 4590.

[62] Liu, A. Wayner, P. C., Jr.; Plawsky, J.; *Appl. Optics* **1994**, *33*, 1223.

[63] Harke, M.; Teppner, R.; Schulz, O.; Motschmann, H.; Orendi, H.; *Rev. Sci. Instr.* **1997**, *68*, 3130.

[64] The width of the pattern is 60 µm.

[65] Harder, P.; Grunze, M.; Dahint, R.; Whitesides, G. M.; Laibinis, P. E.; *J. Phys. Chem. B* **1998**, *102*, 426.

[66] Okano, T., editor; "*Biorelated Polymers and Gels*", Academic Press, San Diego **1998**.

[67] Ding, Z.; Fong, R. B.; Long, C. J.; Stayton, P. S.; Hoffman, A. S.; *Nature* **2001**, *411*, 59.